THE JOURNAL OF PHYSICAL CHEMISTRY LETTERS
A JOURNAL OF THE AMERICAN CHEMICAL SOCIETY

pubs.acs.org/JPCL

Letter

Adsorbed Water Structure on Acrylate-Based Biocompatible Polymer Surface

Saptarsi Mondal, Jooyoun Kang, Kwanghee Park, Jong Min Lim, Jeong-Hyon Ha, Kyungwon Kwak,* and Minhaeng Cho*

Cite This: *J. Phys. Chem. Lett.* 2021, 12, 9275−9282

Read Online

ACCESS | Metrics & More | Article Recommendations | Supporting Information

ABSTRACT: The role of water in the excellent biocompatibility of the acrylate-based polymers widely used for antibiofouling coating material has been realized previously. Here, we report femtosecond mid-infrared pump−probe spectroscopy of the OD stretch band of HOD molecule adsorbed on highly biocompatible poly(2-methoxyethyl) acrylate [PMEA] and poorly biocompatible poly(2-phenoxyethyl) acrylate [PPEA], both of which reveal that there are two water species with significantly different vibrational lifetime. PMEA interacts more strongly with water than PPEA through the H-bonding interaction between carbonyl (C═O) and water. The vibrational lifetime of the OD stretch in PPEA is notably longer by factors of 3 and 7 than those in PMEA and bulk water, respectively. The IR-pump visible-probe photothermal imaging further unravels substantial spatial overlap between polymer CO group and water for hydrated PMEA and a significant difference in surface morphology than those in PPEA, which exhibits the underlying relationships among polymer−water interaction, surface morphology, and biocompatibility.

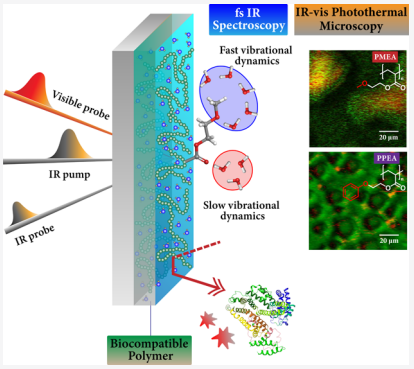

Therapeutic polymers have become widely applicable in the antibiofouling coating of biomedical devices for their exceptional ability to stay inert in the biological environment with very low plasma protein adsorption and platelets adhesion on the polymer surface.[1−4] As structurally similar therapeutic polymers are observed to have significantly different biocompatibility, substantial research has been carried out in the last few decades to understand the factors that affect these polymers' biocompatibility.[5−9] It was revealed that water bound to the polymer surface plays a crucial role in the biocompatibility of acrylate-based polymers.[6,7,10,11] Based on the mobility and the freezing point measurements, the adsorbed water in hydrated polymers was classified into nonfreezing water, intermediate or cold-crystallizable water, and bulk-like water. The nonfreezing water interacts with the surface very strongly and does not freeze even at −100 °C. It has the least mobility and thus very stable on the surface. The intermediate water layer interacts with the nonfreezing water and crystallizes below 0 °C upon heating. Among acrylate-based polymers, poly(2-methoxyethyl acrylate) [PMEA] is several folds higher in biocompatibility as compared to other poly(meth) acrylates [PMAs] such as poly(2-phenoxyethyl acrylate) [PPEA] or poly(ethyl acrylate) [PEA].[12] The superior biocompatibility of PMEA to other PMAs results from the presence of a thick layer of intermediate water on top of the nonfreezing water.[11] Such intermediate water on the surfaces of other PMAs was not observed. Therefore, it was concluded that intermediate water blocking hydrophobic interactions of plasma protein with polymer would be one of the most crucial factors rendering PMEA an excellent biocompatible material.

There are quite a few reports in the literature suggesting that intermediate water is not the sole criterion for the biocompatibility of a given polymer.[6,13] For example, poly(vinyl)alcohol [PVA] or poly(acrylonitrile) [PAN] has a significant amount of intermediate water as compared to PMA, yet they are far less biocompatible than PMA.[6] In some cases, direct hydrogen-bonding interaction of water with the polymer could account for their biocompatibility. For example, aliphatic carbonyl polymers [ACP] and poly(acrylonitrile)-*co*-*N*-2-vinylpyrrolidone [PANcNVP] copolymers have a layer of nonfreezing water that forms a strong hydrogen bond with CO, but no intermediate water on the surfaces of these polymers was detected. Surprisingly, platelet adhesion to those polymers (ACP and PANcNVP) is weaker than that for PVA or PAN.[6] Hence, the role of water and its mode of interaction with the polymer are potentially crucial in understanding the mechanism driving polymer biocompatibility. Furthermore, the classification of water structures into nonfreezing, intermediate, and bulk-like water species is not well-defined at the molecular

Received: July 30, 2021
Published: September 17, 2021

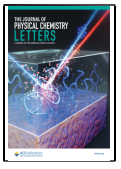

https://doi.org/10.1021/acs.jpclett.1c02491
J. Phys. Chem. Lett. 2021, 12, 9275−9282

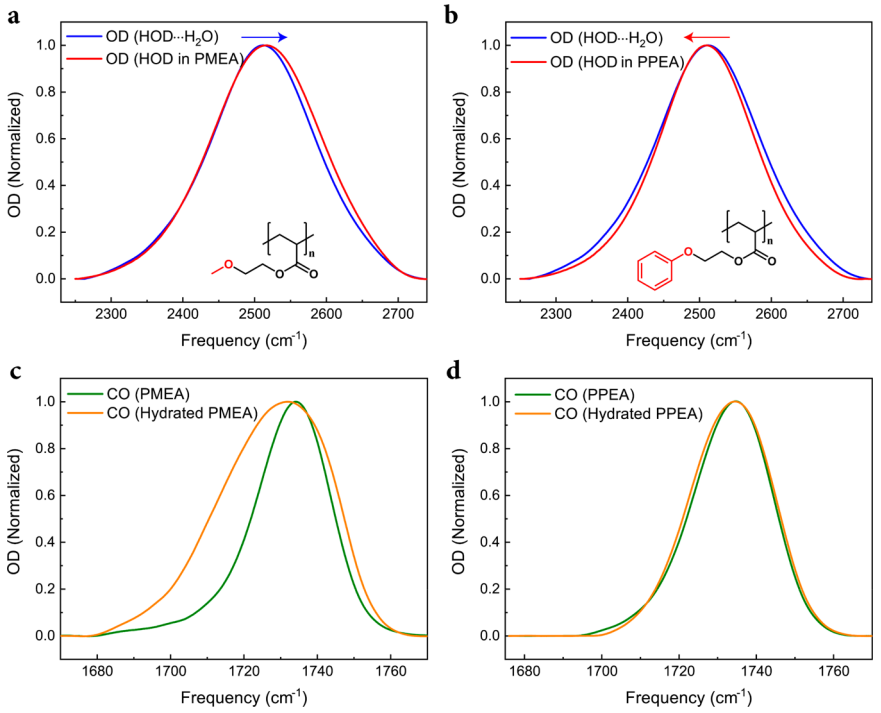

Figure 1. Baseline-corrected and normalized FT-IR spectra of the OD stretch mode of HOD species (a) adsorbed on PMEA and in bulk water and (b) adsorbed on PPEA and, in bulk water, the CO stretch of (c) PMEA with and without adsorbed water [D_2O] and (d) PPEA with and without adsorbed water [D_2O].

level. Additionally, most of the information about the role of water in biocompatibility was obtained from the steady-state spectroscopic and thermodynamic measurements, which overlooked the dynamical aspect of the water H-bond network. Therefore, the water hydration structure and dynamics around highly biocompatible PMEA and poorly biocompatible PPEA polymers investigated with time-resolved spectroscopy are expected to provide a clue to the molecular origin of biocompatibility for these polymers.

This study reports the vibrational relaxation dynamics of the OD stretch mode of HOD adsorbed in PMEA and PPEA using polarization selective mid-IR pump−probe (PP) spectroscopy, which reveals that the water hydration structure and dynamics are significantly different around the PMEA and PPEA surfaces. Furthermore, synchronous 2D correlation spectroscopy (2D-COS) shows a stark difference in the interaction between polymer's CO groups and water molecules. Additionally, we carried out a mid-IR photothermal (MIP) study of the hydrated polymers. In this microscopy technique, the vibrational excitation of the mid-IR pump induces a change in the local temperature and refractive index of the surrounding medium, which deflects the visible probe.[14−17] Since this vibrational/optical microscope allows direct observation of chemical targets in submicrometer lateral resolution, it is suitable for studying the hydrated polymers avoiding any mechanical stress or damages. Here, the MIP microscopy is for the first time used to explore the spatial distributions of water and hydrated polymers, which unravels a stark difference in the spatial overlap of the polymer's CO-rich regions and water-rich regions on the surface of biocompatible polymer. In addition, we show a notable difference in surface morphologies of these two hydrated biocompatible polymers. Furthermore, molecular dynamics (MD) simulations and atoms-in-molecules (AIM) analyses were performed to unveil how the water H-bonding network around the side chain functional groups of the biocompatible polymer varies.

The acrylate-based polymers, PMEA and PPEA, have different functional groups attached to the side chain, e.g., methoxy (−OCH_3) in PMEA and phenoxy (−OPh) in PPEA as shown in Figure 1a,b. First, we carried out Fourier-transform infrared (FT-IR) spectroscopy of the hydrated polymer thin film. The baseline-corrected and normalized FT-IR spectra of the OD stretch of HOD adsorbed on polymer thin films are compared with bulk water (HOD···H_2O) in Figure 1a,b. The broad OD stretch band of HOD···H_2O species (fwhm = 171 cm^{-1}) appears at 2511 cm^{-1} (see Table S1). The OD stretch IR band of HOD in hydrated PMEA is blue-shifted (+6 cm^{-1}), whereas that in PPEA is slightly red-shifted. The fwhm of the FT-IR spectrum of OD increases by 11 cm^{-1} in PMEA, whereas it decreases by 14 cm^{-1} for PPEA compared to the bulk water. A blue-shift of the OD stretch frequency in PMEA indicates a reduction in the number of H-bonded water molecules or a weakening of H-bond strength. The spectral broadening of the OD stretch in PMEA suggests increasing heterogeneity of the hydrogen-bonding network structures. A similar trend was observed previously in HOD molecules interacting with the stern layer of the reverse micelle.[18,19] On the contrary, the OD stretch in PPEA does not change significantly, which indicates that the H-bond environment of water molecules adsorbed on the PPEA surface might be different from that of the PMEA surface.

On the other hand, the CO stretch bands of the polymers are red-shifted upon hydration as compared to those without adsorbed water (Figure 1c,d), which indicates the hydrogen-bonding interaction of CO with water (CO···H_2O). There is a ∼50% increase in the fwhm (+14 cm^{-1}) of the CO band in hydrated PMEA than that of merely 8% (+2 cm^{-1}) for hydrated PPEA.

https://doi.org/10.1021/acs.jpclett.1c02491
J. Phys. Chem. Lett. 2021, 12, 9275−9282

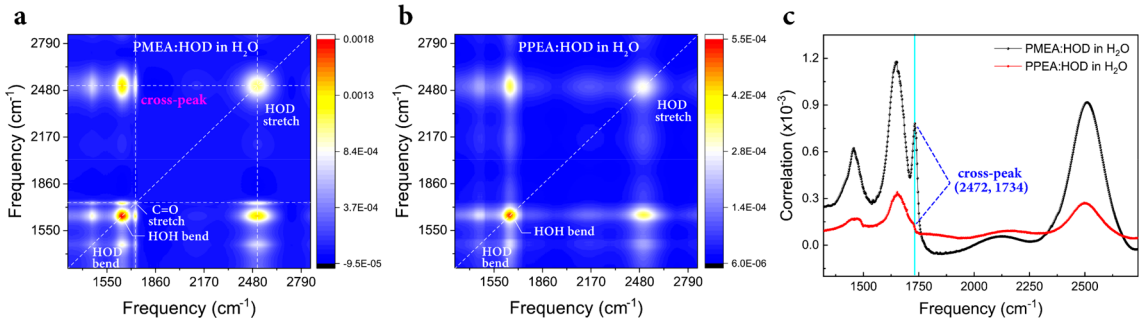

Figure 2. Synchronous 2D-COS analysis of adsorbed water on (a) PMEA, (b) PPEA surfaces and (c) the horizontal slice spectrum at 2472 cm^{-1} for hydrated PMEA and PPEA.

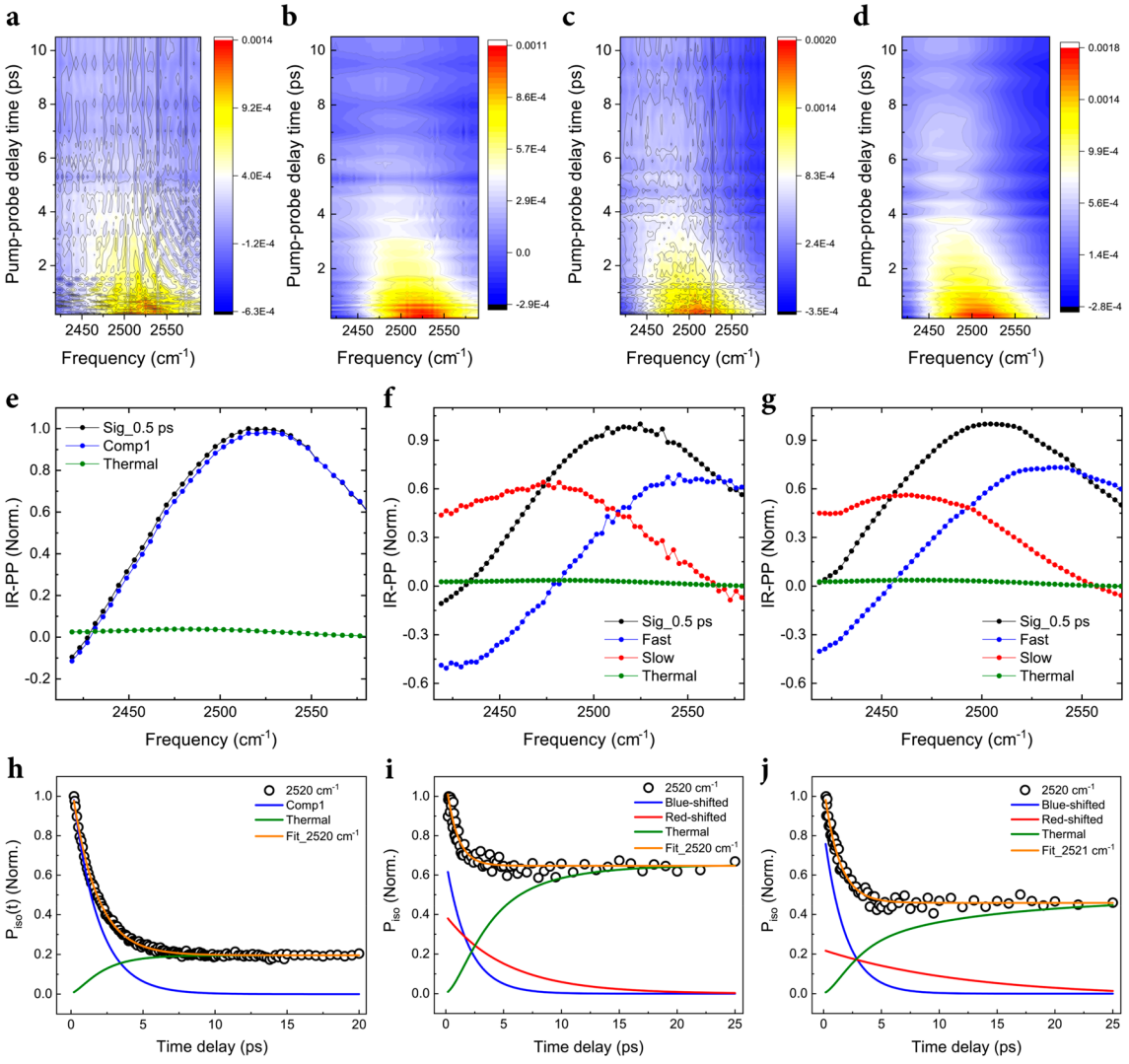

Figure 3. Isotropic IR-PP spectra of the OD stretch mode of HOD in (a) PMEA and (c) PPEA, whereas the corresponding discrete wavelet transform (DWT) corrected signal for (b) PMEA and (d) PPEA after removing the heating contribution. The spectrum of isotropic IR-PP signal of OD of HOD at 0.5 ps delay time in (e) water, (f) PMEA, (g) PPEA, which can be resolved into one decaying component (blue line), and one rising thermal component (green line) for water whereas two decaying components (blue and red line) and one heating component (green line) for hydrated polymer system. The kinetic traces of these components at 2520 cm^{-1} in (h) water, (i) PMEA, and (j) PPEA.

Therefore, this smaller spectral broadening of the CO stretch IR band of hydrated PPEA than that of hydrated PMEA suggests that water interacts weakly with the carbonyl groups of the PPEA compared to those of PMEA. Deconvolution of the OD and CO stretch bands using two Gaussian functions (Figure S1 and Supporting Note 6) show that the area corresponding to CO···DOH species for OD stretch in PMEA is about 1.8 times larger than that of PPEA, whereas for the CO stretch mode, forming H-bonds to the surrounding hydration environment is about 10 times larger than that of PPEA.

https://doi.org/10.1021/acs.jpclett.1c02491
J. Phys. Chem. Lett. 2021, 12, 9275−9282

Further, 2D-COS analysis was performed, which is a useful method for highlighting the characteristic spectral changes of a system upon external perturbation. The primary objective is to investigate if any correlations may exist in the perturbation-induced spectral responses. In addition, 2D-COS analysis reveals the in-phase correlation between different vibrational modes affected similarly due to the same external perturbation, which is otherwise difficult to observe from traditional steady-state spectroscopic experiments like FT-IR. Dynamic variables for the 2D-COS were generated using a time series of FT-IR data collected continuously over several hours for the polymer water systems (see Figure S2). The 2D-COS analyses of hydrated PMEA and PPEA were performed in the spectral range of 1200−2800 cm^{-1} to determine the possible correlations between the OD stretch mode with other normal modes (Figures 2a,b). The crosspeaks in both PMEA and PPEA cases show several strong positive correlations among different modes (see Table S3).

The crosspeak at (2515, 1732) cm^{-1} for PMEA indicates the strong positive correlation between the OD and the CO stretch mode, which can be understood from the strong H-bonding interaction between them. For PPEA, however, the intensity of the crosspeak at (2506, 1734) cm^{-1} is weak and cannot be identified clearly due to the weak H-bonding interaction. Figure 2c represents the horizontal slice spectrum obtained at 2472 cm^{-1} (vertical frequency) for both the hydrated polymers from which the intensity of this cross-peak can be directly compared. Therefore, the 2D-COS analyses essentially reveal that PMEA and PPEA differ significantly in their interaction strengths with water through a CO···DO H-bond.

Next, mid-IR PP measurement of the OD stretch of HOD in hydrated PMEA and PPEA was carried out. The mid-IR PP measurement methods have been successfully employed to understand the dynamic behavior of water in various complex systems before including polymer thin film.[19−22] However, a common challenge of this technique for studying complex heterogeneous material is the appearance of significant pump-induced scattering.[23] A hydrated polymer system is not the exception to this challenge. The transient OD stretch IR PP spectra of the hydrated polymers are severely contaminated with the pump-induced scattering fields. Although the application of widely implemented phase cycling method[24,25] in the time-domain or the Fourier transforms filters in the frequency domain could partly remove the scattered noise from the signal, they often failed to remove scattering enough to perform quantitative analyses. Here we employ a multilevel one-dimensional wavelet decomposition method using discrete wavelet transforms (DWT) to separate the signal from the pump-induced scattering. A detailed description of the DWT method can be found in Supporting Note 8. The accuracy and reliability of the DWT method were validated systematically by applying this method to remove weak and strong scattering associated with the pump−probe signal of CN stretching band in phenyl cyanide (PhCN) dissolved in the ethanol, which is created deliberately by scratching the CaF_2 surface. The method accurately recovers the pump−probe signal without distorting it and can predict the vibrational lifetime of CN in ethanol with merely 2−5% error.

The vibrational lifetime of the IR probe (OD stretch of HOD) is extremely sensitive to the local H-bond environment and has been utilized to probe various systems including peptides, proteins, polymeric surfaces, and Li-ion battery.[18,19,26−29] The lifetime of OD stretch in the bulk water is ∼1.8 ps, but it varies significantly for different polymer surfaces.[20,26,30] The temporal profiles of the isotropic IR-PP signals of the OD stretch of HOD adsorbed in polymers (PMEA and PPEA) and their DWT-corrected profiles are shown in Figure 3a,c and in Figure 3b,d, respectively. These show that the DWT method could successfully remove the pump-induced scattering from the signal. The positive IR-PP signal corresponding to the ground-state bleach (0−1 transition) and the stimulated emission (1−0) of the OD stretch of the HOD molecule was monitored in this study. Additionally, an isotopically diluted solution of 20 vol % HOD in H_2O was used for the pump−probe experiment to implicitly extend the dynamic window of the OD stretch mode beyond ∼0.5 ps.[29] Furthermore, the IR-PP spectra of the OD stretch were successfully corrected for the heating contribution following the kinetic model proposed by the Bakker group[31] (Supporting Note 9). It can be observed that the vibrational energy relaxation of the OD stretch becomes slow when HOD molecules interact with polymer surfaces as compared to those in bulk water. Interestingly, water absorbed in PPEA shows even a slower relaxation than that in PMEA.

For the detailed analysis, the OD stretch IR PP eigenspectra of different HOD species were obtained by performing global fitting analyses considering all the frequencies.[19] The eigenspectrum refers to the frequency-dependent contribution of chemical species with the same vibrational lifetime, shown in Figures 3e−g. The global fitting analysis of the IR PP spectrum of HOD in water shows one decaying component and another in-growing heating signal (Figure 3e). The corresponding kinetic decay traces at 2520 cm^{-1} are plotted in Figure 3h. Furthermore, we analyzed the IR PP time-profiles at the red and blue sides of the isotropic IR PP spectrum of HOD molecules on the polymer surfaces (Figure S11 of Supporting Note 10), which shows that the IR PP signal of the HOD molecule at the red (low-frequency) side of the transient PP signal decays slowly compared to that at the blue (high-frequency) side for both the polymers. This frequency dependence of the OD stretch vibrational lifetime indicates at least two distinctively different water species in the hydrated polymer. Therefore, the isotropic IR-PP signal of the OD stretch mode of HOD was fitted using two exponentially decaying functions and one in-growing heating component (Figures 3i,j). The corresponding eigenspectra are plotted in Figures 3f,g. In addition, the OD stretch IR PP signals at different delay times before and after the correction of the thermal component are compared with each other in Supporting Note 9 (see Figure S10).

The eigenspectra of the OD stretch of HOD for both the polymers show two distinct water species, among which one species is blue-shifted and another is red-shifted compared to the bulk water. Parts i and j of Figure 3 show that the kinetic trace of the blue-shifted water decays faster, whereas that for red-shifted water decays slower. In parts b and c of Figure S12, the vibrational relaxation dynamics of the OD stretch of HOD at 2520 cm^{-1} in pure water are directly compared with those of HOD on biocompatible polymer surfaces. Table 1 shows that the vibrational lifetime of the OD stretch of HOD in pure water is 1.76 ps, which is in excellent agreement with the previously reported value.[32] It should be noted that 20 vol % HOD is used in this study, which shows the same vibrational relaxation time as 5 vol % HOD usually used for time-resolved IR experiments for water. The vibrational lifetime of the fast

https://doi.org/10.1021/acs.jpclett.1c02491
J. Phys. Chem. Lett. 2021, 12, 9275−9282

Table 1. Fitting Parameters of Isotropic Decay Signal of the OD stretch of HOD Species Adsorbed on Various Polymeric Surfaces and in Bulk Water[a]

system	t_1/ps	a_1	t_2/ps	a_2
water	1.76	1.00		
PMEA	1.93	0.54	5.27	0.46
PPEA	1.85	0.71	12.45	0.29

[a]Error not more than ±0.10 ps for t_1 and ±0.40 ps for t_2.

component of OD of HOD species in both the hydrated polymers remains close to 1.8 ps, whereas the slow component varies drastically. The vibrational lifetime of the slow component of the OD stretch in PMEA is 5.3 ps, which is ∼3 times slower than that of the bulk-like water (see Table 1).

Interestingly, the slow component becomes even slower in PPEA with a decay constant of 12.4 ps, which is about ∼7 and ∼2.5 times slower than those of the bulk-like water and water on the PMEA surface, respectively. It should be noted that the eigenspectra and the vibrational relaxation processes of two different HOD species on the polymer surfaces in this study show quite different behaviors as compared to those of HOD molecules in polymer and salt solutions in water studied previously, where it has been shown that the OD stretch modes of HOD molecules with the blue-shifted eigenspectrum have a longer lifetime than those with the red-shifted eigenspectrum in the solution phase.[19,26,32,33] Note that the blue-shifted OD stretch frequency results from a weaker H-bonding interaction of HOD with H-bonding acceptors. In stark contrast, the slowly decaying component in this study is red-shifted, which indicates that the HOD with a strong interaction with the side chain C═O group has a longer lifetime.

Furthermore, the blue-shifted water in the present study appears due to its interaction with the $-OCH_3$ and −OPh groups of the polymer side chain, respectively, for PMEA and PPEA polymer because of the following reasons. Recent studies of interfacial water show that the water OH stretching frequency undergoes a blue-shift for various hydrophobic surfaces.[34−37] Also, vibrational sum-frequency generation spectroscopy of the water interacting with the acrylate-based poly(methyl methacrylate) polymer revealed two water species among which the blue-shifted water interacts with the side chain $-OCH_3$ group of PMMA.[38] Furthermore, IR-PP spectroscopy of water-polyether binary mixture in the water-rich region unveiled that the vibrational lifetime of water associated with the methoxy moiety is ∼2 ps.[39] Interestingly, however, these water molecules close to hydrophobic groups are dynamically inseparable from the bulk water in this study. Therefore, based on the present observations, the blue-shifted water organized around the hydrophobic side chain functional group like $-OCH_3$ (PMEA) and −OPh (PPEA) is assigned to the intermediate water layer. The vibrational lifetime of this intermediate water does not change much in different biocompatible surfaces. In stark contrast, the vibrational relaxation dynamics of the red-shifted water, which interacts with the C═O moiety of the polymer, is substantially slower than that for the blue-shifted water for both PMEA and PPEA and can be assigned to the nonfreezing water layer. Interestingly, the vibrational lifetime of this nonfreezing water (red-shifted water species) changes remarkably based on the biocompatible polymer surface unlike the intermediate water layer (blue-shifted water species) where the vibrational lifetime change is insignificant. Therefore, this result is a clear implication of the underlying relationship of the structure and vibrational dynamics of the interfacial water with the polymer's biocompatibility; however, further experiments are necessary to establish such a relationship more reliably.

The 2D-COS analysis and IR-PP experiment showed that PMEA interacts with water more strongly than PPEA. MIP microscopy was introduced to confirm the interaction of polymer films and water spatially. MIP microscopy provides the chemical sensitivity using mid-IR excitation and submicrometer spatial resolution with a visible probe. With this technique, the spatial distribution of water and polymer can be studied in submicrometer resolution. To investigate the hydration effect on the polymer structure, the OH bending mode of water (1650 cm^{-1}) and CO stretching mode of polymers (1730 cm^{-1}) are targeted for photothermal excitation. Here, it should be noted that the broad and strong absorption band of the water bending mode could contribute to the photothermal image taken with 1730 cm^{-1} IR excitation. Therefore, to obtain the photothermal contrast only for the hydrated carbonyl, we removed the contribution of the water bending mode (see Supporting Note 11 for a detailed description of such correction method).

The CO stretch MIP image (Figure 4, left) of PMEA shows a higher photothermal signal than PPEA, which means that the

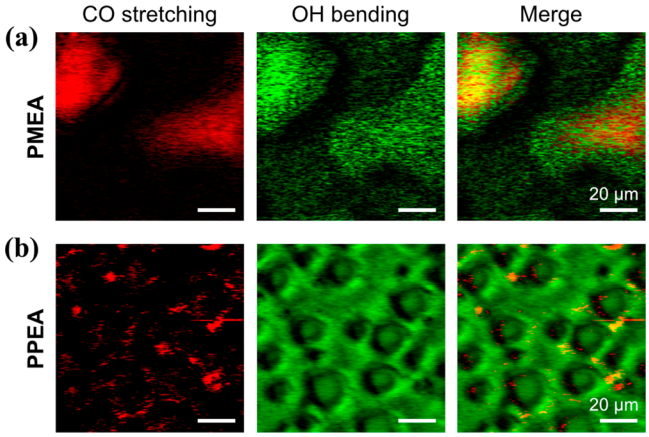

Figure 4. MIP images of the hydrated (a) PMEA and (b) PPEA film. The photothermal effect for water bending (center, green) and CO stretching of polymer (left, red) was measured by the deflection of the visible probe. At 1730 cm^{-1}, both the water bending and CO stretching modes were excited, so the CO stretching MIP image was corrected. Their merged images (right) show the correlation of the adsorbed water and hydrated polymer.

PMEA film has more water-interacting carbonyl moieties than PPEA film. This is because only hydrated polymer can produce a strong photothermal signal due to heating of surrounding water molecules, which leads to a noticeable change in the refractive index, i.e., photothermal effect. The MIP images of PMEA and PPEA clearly show that the two polymers have quite different water environments. Although both polymers contain carbonyl groups that can be excited by a 1730 cm^{-1} IR beam, the PMEA is in a high-level hydration state because its photothermal signal is much stronger than that of PPEA (Supporting Note 12). More specifically, the CO stretch MIP image of PMEA polymer shows a distinct localization feature of the hydrated polymer. Furthermore, the water bend and the CO stretch MIP images overlap in lateral space, indicating that

https://doi.org/10.1021/acs.jpclett.1c02491
J. Phys. Chem. Lett. 2021, 12, 9275−9282

most adsorbed water molecules are close to the C═O groups of PMEA (Figure 4a). Although the OH bend MIP image of the PPEA film exhibits a broad spatial distribution of water, water molecules do not specifically interact with the carbonyl moieties of PPEA (Figure 4b). In PPEA film, the CO stretch MIP signal is comparatively weak, and there is no strong correlation in the spatial distributions of the water bending and CO stretch MIP images. Indeed, our photothermal imaging studies of two vibrational modes, i.e., water bending and polymer CO stretch, are consistent with the 2D-COS analysis results, indicating that the intermolecular interaction between water and carbonyl group of PMEA is stronger than that of PPEA.

We found that the surface morphologies of the hydrated PMEA and PPEA films are notably different. Both the adsorbed water and the hydrated carbonyl of PMEA usually make broad lumps (Figure 4a), whereas the adsorbed water on PPEA has a clot-like structure (Figure 4b). MIP images measured at different positions show similar patterns (Figure S17 and Supporting Note 13). It implies that the morphologies of hydrated polymers appearing from their interaction with water molecules may be related to the biocompatible behavior of the respective polymer. In addition, considering that the distribution and amplitude of the MIP signal do not change even after multiple measurements (Figure S17), we confirm that the measurement itself does not damage the hydrated polymer samples.

Furthermore, position-restrained all-atom MD simulation and AIM analyses were carried out to understand water organization around the side chain functional group and the nature of the H-bonding interaction for the first solvation shell of PMEA and PPEA monomer and hexamer (see Supporting Notes 14 and 15 for details). It is observed that more water molecules prefer to interact with the hydrophilic CO group for PMEA than PPEA, with strong H-bonding interaction accounting for the water with red-shifted OD frequency. On the contrary, a greater number of water molecules organize themselves around the phenyl group of PPEA rather than the methyl moiety of PMEA through weak C—H···O_w noncovalent interaction, which disrupts the cooperative water H-bonding network and gives rise to an OD-frequency blue-shift as observed in the transient IR PP spectra of both the polymers. Therefore, MD simulations coupled with AIM analysis reveal that biocompatible polymer PMEA could have significantly different hydration structures and noncovalent interactions with surrounding water molecules than the poorly biocompatible PPEA polymer, which probably plays a crucial role in altering the vibrational dynamics of water. Therefore, substantially longer vibrational dynamics of the nonfreezing water in PPEA could be related to the reduced vibrational density of states of water, which steers the relaxation process predominantly to go through the nonradiative decay channel of CO···water H-bond over the intramolecular coupling of the donor OD stretch with the acceptor modes. However, comparatively faster vibrational dynamics of the nonfreezing water in PMEA probably relax through both CO···water H-bonding interaction and intramolecular coupling of donor and acceptor modes, including low-frequency vibrations or combination bands.

In summary, two acrylate-based biocompatible polymers were investigated using polarization-selective mid-IR PP spectroscopy, 2D-COS analysis, MIP imaging technique coupled with MD simulations, and AIM analysis to report the observation of how water molecule interacts with different biocompatible polymer surface. The vibrational relaxation dynamics of the OD stretch of HOD unveil the presence of two distinct water species in the hydrated PMEA and PPEA polymer films. The water molecules with a short vibrational lifetime of ∼1.8 ps are blue-shifted in the OD frequency and can be assigned to the intermediate water, which interacts with the hydrophobic moiety through weak to moderately strong noncovalent interactions. However, the vibrational lifetime of the other water species having a longer vibrational lifetime varies substantially on different biocompatible surfaces. This OD frequency-red-shifted water can be assigned to the nonfreezing water H-bonded to the CO group of the polymer and exhibits a significantly slow vibrational relaxation for PPEA. The present work thus reveals that the chemical nature of the side chain functional group and the extent of cooperative water H-bonding network control the vibrational dynamics of the nonfreezing water, which may have some crucial role to play in the biocompatibility of the acrylate-based polymer. Furthermore, the MIP imaging study reveals a significant difference in the surface morphology of the biocompatible polymers, which could be essential to understand the interaction of water with the polymer as well. Thus, we hope that the present study will enrich our understanding of the role of the specific interaction of water with the side chain functional group of the biocompatible polymer essential for developing the next-generation biocompatible materials.

■ ASSOCIATED CONTENT

Supporting Information

The Supporting Information is available free of charge at https://pubs.acs.org/doi/10.1021/acs.jpclett.1c02491.

Sample preparation, experimental techniques, deconvolution of the FT-IR spectra, denoising of the transient pump−probe spectra using multilevel discrete wavelet transform method, heating contribution correction, frequency-dependent vibrational relaxation dynamics, MIP imaging study, MD simulation, and AIM analysis (PDF)

■ AUTHOR INFORMATION

Corresponding Authors

Kyungwon Kwak − *Center for Molecular Spectroscopy and Dynamics, Institute for Basic Science (IBS), Seongbuk-gu, Seoul 02841, Republic of Korea; Department of Chemistry, Korea University, Seongbuk-gu, Seoul 02841, Republic of Korea;* orcid.org/0000-0003-1680-0996; Email: kkwak@korea.ac.kr

Minhaeng Cho − *Center for Molecular Spectroscopy and Dynamics, Institute for Basic Science (IBS), Seongbuk-gu, Seoul 02841, Republic of Korea; Department of Chemistry, Korea University, Seongbuk-gu, Seoul 02841, Republic of Korea;* orcid.org/0000-0003-1618-1056; Email: mcho@korea.ac.kr

Authors

Saptarsi Mondal − *Center for Molecular Spectroscopy and Dynamics, Institute for Basic Science (IBS), Seongbuk-gu, Seoul 02841, Republic of Korea; Department of Chemistry, Korea University, Seongbuk-gu, Seoul 02841, Republic of Korea;* orcid.org/0000-0003-1140-9322

https://doi.org/10.1021/acs.jpclett.1c02491
J. Phys. Chem. Lett. 2021, 12, 9275−9282

Jooyoun Kang − *Center for Molecular Spectroscopy and Dynamics, Institute for Basic Science (IBS), Seongbuk-gu, Seoul 02841, Republic of Korea; Department of Chemistry, Korea University, Seongbuk-gu, Seoul 02841, Republic of Korea*

Kwanghee Park − *Center for Molecular Spectroscopy and Dynamics, Institute for Basic Science (IBS), Seongbuk-gu, Seoul 02841, Republic of Korea; Department of Chemistry, Korea University, Seongbuk-gu, Seoul 02841, Republic of Korea*

Jong Min Lim − *Center for Molecular Spectroscopy and Dynamics, Institute for Basic Science (IBS), Seongbuk-gu, Seoul 02841, Republic of Korea; Department of Chemistry, Korea University, Seongbuk-gu, Seoul 02841, Republic of Korea;* orcid.org/0000-0003-0311-1032

Jeong-Hyon Ha − *Korea Basic Science Institute, Natural Science Campus, Korea University, Seongbuk-gu, Seoul 02841, Republic of Korea*

Complete contact information is available at: https://pubs.acs.org/10.1021/acs.jpclett.1c02491

Notes

The authors declare no competing financial interest.

■ ACKNOWLEDGMENTS

This work was supported by the Institute for Basic Science (IBS-R023-D1) (M.C.) and the National Research Foundation of Korea (NRF) grant funded by the Korean government (MSIT) (NRF-2020R1A2C2010675) (K.K.).

■ REFERENCES

(1) Ishihara, K. Blood-Compatible Surfaces with Phosphorylcholine-Based Polymers for Cardiovascular Medical Devices. *Langmuir* **2019**, *35* (5), 1778−1787.

(2) Kobayashi, S.; Wakui, M.; Iwata, Y.; Tanaka, M. Poly(ω-methoxyalkyl acrylate)s: Nonthrombogenic Polymer Family with Tunable Protein Adsorption. *Biomacromolecules* **2017**, *18* (12), 4214−4223.

(3) Ko, D. Y.; Patel, M.; Jung, B. K.; Park, J. H.; Jeong, B. Phosphorylcholine-Based Zwitterionic Biocompatible Thermogel. *Biomacromolecules* **2015**, *16* (12), 3853−3862.

(4) Iwasaki, Y.; Ishihara, K. Phosphorylcholine-containing polymers for biomedical applications. *Anal. Bioanal. Chem.* **2005**, *381* (3), 534−546.

(5) Fukushima, K.; Tsai, M.-Y.; Ota, T.; Haga, Y.; Matsuzaki, K.; Inoue, Y.; Tanaka, M. Evaluation of the hemocompatibility of hydrated biodegradable aliphatic carbonyl polymers with a subtle difference in the backbone structure based on the intermediate water concept and surface hydration. *Polym. J.* **2015**, *47*, 469.

(6) Bag, M. A.; Valenzuela, L. M. Impact of the Hydration States of Polymers on Their Hemocompatibility for Medical Applications: A Review. *Int. J. Mol. Sci.* **2017**, *18* (8), 1422.

(7) Morita, S.; Tanaka, M. Effect of Sodium Chloride on Hydration Structures of PMEA and P(MPC-r-BMA). *Langmuir* **2014**, *30* (35), 10698−10703.

(8) Tanaka, M.; Mochizuki, A.; Shiroya, T.; Motomura, T.; Shimura, K.; Onishi, M.; Okahata, Y. Study on kinetics of early stage protein adsorption on poly(2-methoxyethylacrylate) (PMEA) surface. *Colloids Surf., A* **2002**, *203* (1), 195−204.

(9) Tanaka, M.; Mochizuki, A.; Ishii, N.; Motomura, T.; Hatakeyama, T. Study of Blood Compatibility with Poly(2-methoxyethyl acrylate). Relationship between Water Structure and Platelet Compatibility in Poly(2-methoxyethylacrylate-co-2-hydroxyethylmethacrylate). *Biomacromolecules* **2002**, *3* (1), 36−41.

(10) Sato, K.; Kobayashi, S.; Kusakari, M.; Watahiki, S.; Oikawa, M.; Hoshiba, T.; Tanaka, M. The Relationship Between Water Structure and Blood Compatibility in Poly(2-methoxyethyl Acrylate) (PMEA) Analogues. *Macromol. Biosci.* **2015**, *15* (9), 1296−1303.

(11) Tanaka, M.; Hayashi, T.; Morita, S. The roles of water molecules at the biointerface of medical polymers. *Polym. J.* **2013**, *45*, 701.

(12) Tanaka, M.; Motomura, T.; Kawada, M.; Anzai, T.; Yuu, K.; Shiroya, T.; Shimura, K.; Onishi, M.; Akira, M. Blood compatible aspects of poly(2-methoxyethylacrylate) (PMEA)—relationship between protein adsorption and platelet adhesion on PMEA surface. *Biomaterials* **2000**, *21* (14), 1471−1481.

(13) Tada, S.; Inaba, C.; Mizukami, K.; Fujishita, S.; Gemmei-Ide, M.; Kitano, H.; Mochizuki, A.; Tanaka, M.; Matsunaga, T. Anti-Biofouling Properties of Polymers with a Carboxybetaine Moiety. *Macromol. Biosci.* **2009**, *9* (1), 63−70.

(14) Lim, J. M.; Park, C.; Park, J.-S.; Kim, C.; Chon, B.; Cho, M. Cytoplasmic Protein Imaging with Mid-Infrared Photothermal Microscopy: Cellular Dynamics of Live Neurons and Oligodendrocytes. *J. Phys. Chem. Lett.* **2019**, *10* (11), 2857−2861.

(15) Zhang, D.; Li, C.; Zhang, C.; Slipchenko, M. N.; Eakins, G.; Cheng, J.-X. Depth-resolved mid-infrared photothermal imaging of living cells and organisms with submicrometer spatial resolution. *Sci. Adv.* **2016**, *2* (9), e1600521.

(16) Mërtiri, A.; Jeys, T.; Liberman, V.; Hong, M. K.; Mertz, J.; Altug, H.; Erramilli, S. Mid-infrared photothermal heterodyne spectroscopy in a liquid crystal using a quantum cascade laser. *Appl. Phys. Lett.* **2012**, *101* (4), 044101.

(17) Furstenberg, R.; Kendziora, C.; Papantonakis, M.; Nguyen, V.; McGill, R. A. Chemical imaging using infrared photothermal microspectroscopy. *Proc. SPIE* **2012**, *8374*, 837411.

(18) Kundu, A.; Verma, P. K.; Cho, M. Water Structure and Dynamics in the Stern Layer of Micelles: Femtosecond Mid-Infrared Pump-Probe Spectroscopy Study. *J. Phys. Chem. B* **2019**, *123* (25), 5238−5245.

(19) Lim, J.; Park, K.; Lee, H.; Kim, J.; Kwak, K.; Cho, M. Nanometric Water Channels in Water-in-Salt Lithium Ion Battery Electrolyte. *J. Am. Chem. Soc.* **2018**, *140* (46), 15661−15667.

(20) Kim, H.; Cho, M. Infrared Probes for Studying the Structure and Dynamics of Biomolecules. *Chem. Rev.* **2013**, *113* (8), 5817−5847.

(21) Yan, C.; Kramer, P. L.; Yuan, R.; Fayer, M. D. Water Dynamics in Polyacrylamide Hydrogels. *J. Am. Chem. Soc.* **2018**, *140* (30), 9466−9477.

(22) Nishida, J.; Breen, J. P.; Lindquist, K. P.; Umeyama, D.; Karunadasa, H. I.; Fayer, M. D. Dynamically Disordered Lattice in a Layered Pb-I-SCN Perovskite Thin Film Probed by Two-Dimensional Infrared Spectroscopy. *J. Am. Chem. Soc.* **2018**, *140* (31), 9882−9890.

(23) Spector, I. C.; Olson, C. M.; Huber, C. J.; Massari, A. M. Simple fully reflective method of scatter reduction in 2D-IR spectroscopy. *Opt. Lett.* **2015**, *40* (8), 1850−1852.

(24) Kwak, K.; Rosenfeld, D. E.; Chung, J. K.; Fayer, M. D. Solute−Solvent Complex Switching Dynamics of Chloroform between Acetone and Dimethylsulfoxide−Two-Dimensional IR Chemical Exchange Spectroscopy. *J. Phys. Chem. B* **2008**, *112* (44), 13906−13915.

(25) Moilanen, D. E.; Piletic, I. R.; Fayer, M. D. Water Dynamics in Nafion Fuel Cell Membranes: The Effects of Confinement and Structural Changes on the Hydrogen Bond Network. *J. Phys. Chem. C* **2007**, *111* (25), 8884−8891.

(26) Kundu, A.; Verma, P. K.; Cho, M. Role of Solvent Water in the Temperature-Induced Self-Assembly of a Triblock Copolymer. *J. Phys. Chem. Lett.* **2017**, *8* (13), 3040−3047.

(27) Rezus, Y. L. A.; Bakker, H. J. Orientational dynamics of isotopically diluted H2O and D2O. *J. Chem. Phys.* **2006**, *125* (14), 144512.

(28) Rezus, Y. L. A.; Bakker, H. J. On the orientational relaxation of HDO in liquid water. *J. Chem. Phys.* **2005**, *123* (11), 114502.

(29) Lawrence, C. P.; Skinner, J. L. Vibrational spectroscopy of HOD in liquid D2O. III. Spectral diffusion, and hydrogen-bonding and rotational dynamics. *J. Chem. Phys.* **2003**, *118* (1), 264−272.
(30) Verma, P. K.; Lee, H.; Park, J.-Y.; Lim, J.-H.; Maj, M.; Choi, J.-H.; Kwak, K.-W.; Cho, M. Modulation of the Hydrogen Bonding Structure of Water by Renal Osmolytes. *J. Phys. Chem. Lett.* **2015**, *6* (14), 2773−2779.
(31) Post, S. T. v. d.; Bakker, H. J. The combined effect of cations and anions on the dynamics of water. *Phys. Chem. Chem. Phys.* **2012**, *14* (18), 6280−6288.
(32) Kundu, A.; Kwak, K.; Cho, M. Water Structure at the Lipid Multibilayer Surface: Anionic Versus Cationic Head Group Effects. *J. Phys. Chem. B* **2016**, *120* (22), 5002−5007.
(33) Kundu, A.; Verma, P. K.; Ha, J.-H.; Cho, M. Studying Water Hydrogen-Bonding Network near the Lipid Multibilayer with Multiple IR Probes. *J. Phys. Chem. A* **2017**, *121* (7), 1435−1441.
(34) Tomobe, K.; Yamamoto, E.; Kojić, D.; Sato, Y.; Yasui, M.; Yasuoka, K. Origin of the blueshift of water molecules at interfaces of hydrophilic cyclic compounds. *Sci. Adv.* **2017**, *3* (12), e1701400.
(35) Davis, J. G.; Rankin, B. M.; Gierszal, K. P.; Ben-Amotz, D. On the cooperative formation of non-hydrogen-bonded water at molecular hydrophobic interfaces. *Nat. Chem.* **2013**, *5* (9), 796−802.
(36) Davis, J. G.; Gierszal, K. P.; Wang, P.; Ben-Amotz, D. Water structural transformation at molecular hydrophobic interfaces. *Nature* **2012**, *491* (7425), 582−585.
(37) Scatena, L. F.; Brown, M. G.; Richmond, G. L. Water at Hydrophobic Surfaces: Weak Hydrogen Bonding and Strong Orientation Effects. *Science* **2001**, *292* (5518), 908−912.
(38) Myalitsin, A.; Ghosh, S.; Urashima, S.-h.; Nihonyanagi, S.; Yamaguchi, S.; Aoki, T.; Tahara, T. Structure of water and polymer at the buried polymer/water interface unveiled using heterodyne-detected vibrational sum frequency generation. *Phys. Chem. Chem. Phys.* **2020**, *22* (29), 16527−16531.
(39) Fenn, E. E.; Moilanen, D. E.; Levinger, N. E.; Fayer, M. D. Water Dynamics and Interactions in Water−Polyether Binary Mixtures. *J. Am. Chem. Soc.* **2009**, *131* (15), 5530−5539.

https://doi.org/10.1021/acs.jpclett.1c02491
J. Phys. Chem. Lett. 2021, 12, 9275−9282